



Adsorption studies of Cu(II) on Boston fern (*Nephrolepis exaltata* Schott cv. *Bostoniensis*) leaves

Rifaqat Ali Khan Rao¹ · Umra Khan¹

Received: 27 May 2015 / Accepted: 19 January 2016

© The Author(s) 2016. This article is published with open access at Springerlink.com

Abstract Adsorption studies were done on Boston fern leaves for the effective removal of Cu(II) ions from aqueous solution. It has been tested for the first time for heavy metal adsorption from aqueous solution. This promising material has shown remarkable adsorption capacity towards Cu(II) ions which confirm its novelty, ease of availability, non-toxic nature, cheapness, etc., and give the main innovation to the present study. The adsorbent was analyzed by FT-IR, SEM and EDS. The effect of pH, contact time, initial metal ion concentration and temperature on the adsorption was investigated using batch process to optimize conditions for maximum adsorption. The adsorption of Cu(II) was maximum (96 %) at pH 4. The experimental data were analyzed by Langmuir, Freundlich and Tempkin isotherms. The kinetic studies of Cu(II) were carried out at room temperature (30 °C) in the concentration range 10–100 mg L⁻¹. The data obtained fitted well with the Langmuir isotherm and pseudo-second-order kinetics model. The maximum adsorption capacity (q_m) obtained from Langmuir adsorption isotherm was found to be 27.027 mg g⁻¹ at 30 °C. The process was found to be exothermic and spontaneous in nature. The breakthrough and exhaustive capacities were found to be 12.5 and 37.5 mg g⁻¹, respectively. Desorption studies showed that 93.3 % Cu(II) could be desorbed with 0.1 M HCl by continuous mode.

Keywords Adsorption · Boston fern · Isotherms · Thermodynamic · Kinetics · Breakthrough capacity

Introduction

Heavy metal presence in the environment has several adverse health effects on a variety of living organisms. Ingestion of these metals by humans in excessive amount can cause accumulative poisoning, cancer, nervous system damage and ultimately death (Corapcioglu and Huang 1987; Issabeayev et al. 2006). Copper is essential for human life but excess intake can cause anemia, liver damage, kidney damage, stomach and intestinal irritation. The WHO permissible limit of Cu(II) for drinking water is 2 mg L⁻¹ and that for wastewater and industrial effluents is 3 mg L⁻¹. Several remediation methods like chemical precipitation, lime coagulation, reverse osmosis, ion exchange and solvent extraction have been developed and used but they either are ineffective or expensive (Ahalya et al. 2003). Heavy metal removal processes should be simple, effective and inexpensive. Exploration of new and cheap methods of metal ions removal from industrial wastewater is gaining continuous research impetus with adsorption considered to be most economically viable method.

Metals can be removed from solution only when they are aptly immobilized, the procedure of metal removal from aqueous solutions often leading to effectively concentrating the metal. Adsorption makes the eventual recovery of metals easier and economical. A number of adsorbent materials have been studied for their ability to remove heavy metals and they have been sourced from natural materials and biological wastes of industrial processes (Igbinosa and Okah 2009). Adsorption in the natural

✉ Rifaqat Ali Khan Rao
rakrao1@rediffmail.com

Umra Khan
Umrakhan.amu@gmail.com

¹ Environmental Research Laboratory, Department of Applied Chemistry, Faculty of Engineering and Technology, Aligarh Muslim University, Aligarh 202002, UP, India

or uncontrolled situation typically involves a combination of active and passive transport mechanisms starting with the diffusion of the metal ion to the surface of the adsorbent (Donmez et al. 1999). A number of plant materials or agricultural residues have been used largely as adsorbents for the removal of Cu(II) from water and wastewater (Bulut and Tez 2007). These include peat (Lodenius et al. 1983), bark (Vanquez et al. 2002), cellulose (Navarro et al. 1996), lignite (Eligwe et al. 1999), coconut husks (Hasany et al. 2003), rice husk (Khalid et al. 1999), vegetables (Ponomarev et al. 1997), tea leaves (Kiyohara et al. 2003), baggase fly ash (Gupta and Ali 2000), peanut hull carbon (Periasamy and Namasivayam 1996), pine bark (Al-Asheh et al. 2003), sphagnum moss peat (McKay 2000) etc.

Different aquatic (Donmez et al. 1999; Taghi Ganji et al. 2005; Antunes et al. 2001) and tree ferns (Yuh-shan 2002; Ho et al. 2002) have also been widely used for removal of metal ions from aqueous solutions. In the present study, a new adsorbent Boston fern (BF), *Nephrolepis exaltata* cv. *Bostoniensis* has been used to remove copper from aqueous solution as an alternative to the conventional treatment approaches. It is a very popular ornamental plant, often grown in hanging baskets or similar conditions and more tolerant to dry conditions and easy to propagate.

Materials and methods

Adsorbent

Boston fern was acquired from Aligarh Muslim University campus, Aligarh. The leaves of the plant were washed several times with double distilled water (DDW) to remove dirt and dust and then air dried. The adsorbent was crushed and sieved with 50–100 mesh size after drying and sealed in bottle for further use.

Adsorbent solution

Stock solution of Cu(II) was prepared (1000 mg L⁻¹) by dissolving 0.95 g of Cu(NO₃)₂·3H₂O (AR grade) in DDW.

Instruments and apparatus

Perkin Elmer 1800 model IR spectrophotometer operating at a frequency range of 400–4000 cm⁻¹ was used to record the FT-IR spectra of the adsorbent material using KBr pellets. GSM 6510LV Scanning electron microscope was used for scanning electron microscopy and electron diffraction scattering (SEM/EDS) analysis. The concentration of metal ions in the solution was measured by a flame atomic absorption spectrophotometer model GBC

902 (Australia). Elico Li 120 pH meter was used to measure the pH of the solutions.

Adsorption studies

Adsorption studies were carried out using batch process. 0.2 g of adsorbent was put in a conical flask in which 20 mL solution of Cu(II) of desired concentration was added. The mixture was shaken in a shaker incubator and then filtered. Atomic absorption spectrophotometer (AAS) was used to determine the amount of Cu(II) in the filtrate. The amount of Cu(II) adsorbed was calculated by subtracting the final concentration of Cu(II) from the initial concentration. The adsorption capacity, q_e was obtained using the Eq. (1):

$$q_e = \frac{(C_o - C_e) \times V(L)}{W(g)} \quad (1)$$

Where C_o and C_e (mg L⁻¹) are the initial and final concentrations of metal ions, V (L) is the volume of the solution taken and W (g) is the weight of adsorbent.

Effect of pH

pH ranging from 1.0 to 10.0 was used to study the effect of hydrogen ion concentration on the adsorption of Cu(II). 20 mL solution containing 50 mg L⁻¹ Cu(II) was taken in a series of 250 mL conical flasks. 0.1 M HCl or 0.1 M NaOH solution was added in each flask to adjust the pH of the solution. 0.2 g adsorbent was then added in each flask. The flasks were then shaken in a shaker incubator for 24 h. The solution was then filtered and filtrate was analyzed for Cu(II) by AAS. The amount of Cu(II) adsorbed at each pH value was then calculated as described above. The final pH (pH_f) or equilibrium pH after adsorption of Cu(II) was also recorded. Same procedure as described above was repeated to study the effect of electrolyte on the adsorption of Cu(II) at different pH values by preparing 50 mg L⁻¹ Cu(II) solution in 0.1 M KNO₃. The adsorption process and point of zero charge are greatly affected in the presence of electrolyte (Tripathy and Kanungo 2005). The effect of electrolyte was studied along with pH and for this 0.1 M KNO₃ was used as electrolyte.

Point of zero charge (pH_{zpc})

Solid addition method was used to determine the zero surface charge (Elangovan et al. 2008). 16 mL of 0.1 M KNO₃ solution was added to a series of 100 mL conical flasks. First, pH of the solution in each flask was approximately adjusted from 1 to 10 by either adding 0.1 M HCl or 0.1 M NaOH. The final volume was then adjusted to

20 mL by adding 0.1 M KNO_3 solution. The solutions were kept for 3 h and then pH of these solutions was measured precisely. 0.2 g adsorbent was then added in each flask and flasks were shaken periodically and kept for 24 h. The final pH (pH_f) was then recorded. The difference in pH, (ΔpH) = $\text{pH}_i - \text{pH}_f$ was plotted against pH_i and the point of intersection with abscissa of the resulting curve, where $\Delta\text{pH} = 0$, gave the pH_{zpc} .

Effect of time

A series of 250 mL flasks each containing 0.2 g adsorbent and 20 mL solution of known Cu(II) concentration (10, 30, 50, 70 and 100 mg L^{-1}) were used to carry out contact time studies. The flasks were shaken in a shaker incubator. The solutions of the flasks were then filtered at predetermined time intervals (5, 10, 15, 30, 60, 120 min) and the concentration of the supernatant solution from each flask was then determined.

Breakthrough capacity

0.2 g of adsorbent was packed in a glass column (0.6 cm internal diameter) with glass wool support. One liter of 50 mg L^{-1} initial concentration Cu(II) solution was then passed through the column at a flow rate of 1 mL min^{-1} . The effluent was collected in 10 mL fractions (100 mL) in the beginning and then 50 mL fractions. AAS was used to determine the amount of Cu(II) in each fraction and breakthrough curve was obtained by plotting C/C_0 versus volume of effluent (mL).

Desorption studies

Any excess of Cu(II) in the exhausted column (after breakthrough capacity) was removed by washing several times with DDW. The adsorbed Cu(II) was desorbed by passing 0.1 M HCl solution through the column with a flow rate of 1 mL min^{-1} . The effluent was collected in 10 mL fractions and the amount of Cu(II) in each fraction was determined.

Results and discussions

Adsorption of heavy metals

The % adsorption of Cu(II), Cr(VI), Pb(II), Cd(II) and Ni(II) onto Boston fern at pH 6.5 is shown in Fig. 1. The % adsorption was found in the order of $\text{Cu(II)} > \text{Pb(II)} > \text{Ni(II)} > \text{Cd(II)} > \text{Cr(VI)}$. Since Cu(II) showed maximum adsorption hence it was selected for further studies.

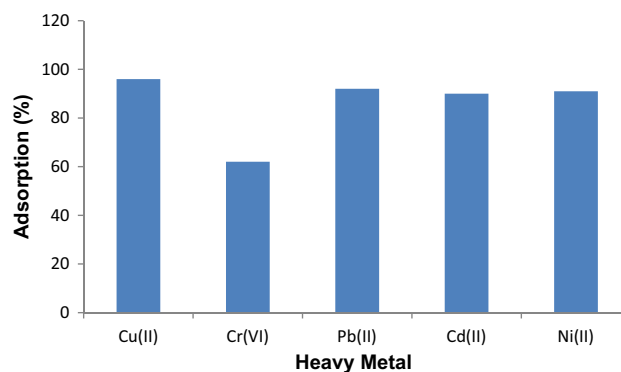


Fig. 1 Percent adsorption of heavy metal ions from aqueous solution onto BF (conditions; adsorbent = 0.2 g, heavy metal = 50 mg L^{-1} each, temperature = 30 °C)

Characterization of adsorbent

Scanning electron microscope (SEM) analysis

Scanning electron microscope (SEM) was used to analyze the surface of the adsorbent before and after adsorption of Cu(II). The particles on the surface before adsorption were found to be uneven, porous, and asymmetric rod like structures. The irregularities in shapes of the particles present on the surface of the adsorbent have affinity for binding internally and thus adsorb more metal ions is the basic principle of adsorption. After the adsorption of Cu(II), the vacant sites appeared to be filled showing adsorption of metal ions on the surface as shown in Fig. 2a, b. Carbon and oxygen were shown as major constituents in EDS peaks as indicated by high values of weight % (Table 1). Appearance of Cu peaks in EDS spectra showed successful adsorption Fig. 3a, b.

FT-IR analysis

The FT-IR spectra of Boston fern [before and after Cu(II) adsorption] are shown in Fig. 4a, b, respectively. To determine the possibility of interactions between the functional groups present on the surface of adsorbent and Cu(II) ions, FT-IR analysis was carried out. The spectra showed ionisable functional groups (carboxylic and hydroxyl) which interacted with metal ions. The broad spectral band at 3391.1 cm^{-1} was assigned to (OH) vibration of hydrogen-bonded hydroxyl functional groups. The two intense peaks at 2919.2–2850.2 cm^{-1} were due to asymmetric and symmetric stretching (C–H) of aliphatic compounds. A characteristic peak at 1735.2 cm^{-1} was assigned to (C=O) band vibration of carbonyl group and peak at 1628.1 cm^{-1} indicates the presence of (C=C) groups. The peak present at 1244.2 indicate (C=C) aromatic bending and peaks at 1059.1 and 1035.1 cm^{-1} were

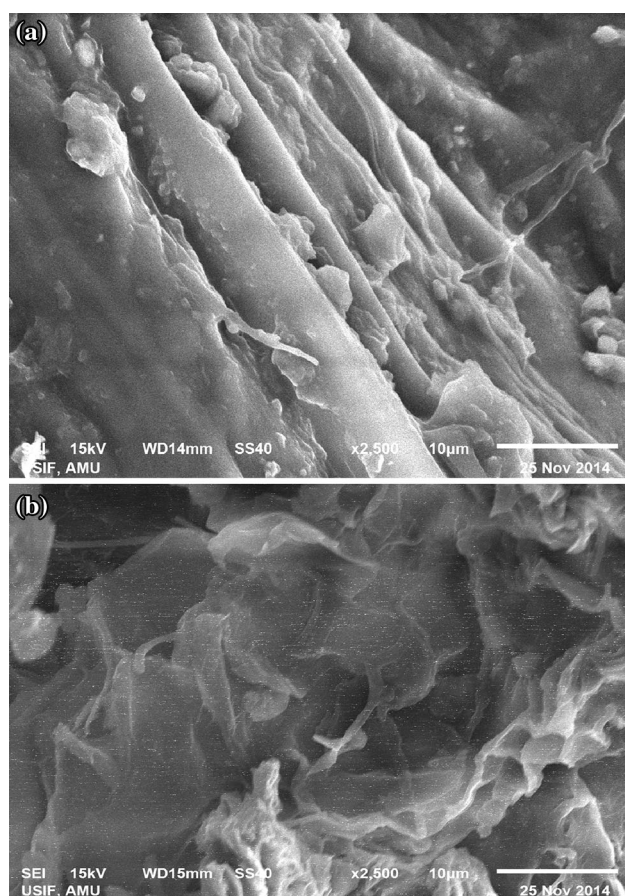


Fig. 2 SEM micrograph of BF **a** before and **b** after adsorption of Cu(II) (magnification: $\times 2500$)

due to C–C stretching. The broad peaks at 619.2 and 534.2 represented C–H bending. The shifting of peaks from 3391.1 to 3397.2, 1244.2 to 1246.3 and 534.2 to 537.4 cm^{-1} were due to binding of Cu(II) ions with carboxyl and hydroxyl group (Sheng et al. 2004).

Effect of contact time on adsorption of Cu(II) at different initial concentrations

To overcome all mass transfer resistance of metal ions between the aqueous and solid phase, the initial metal ion

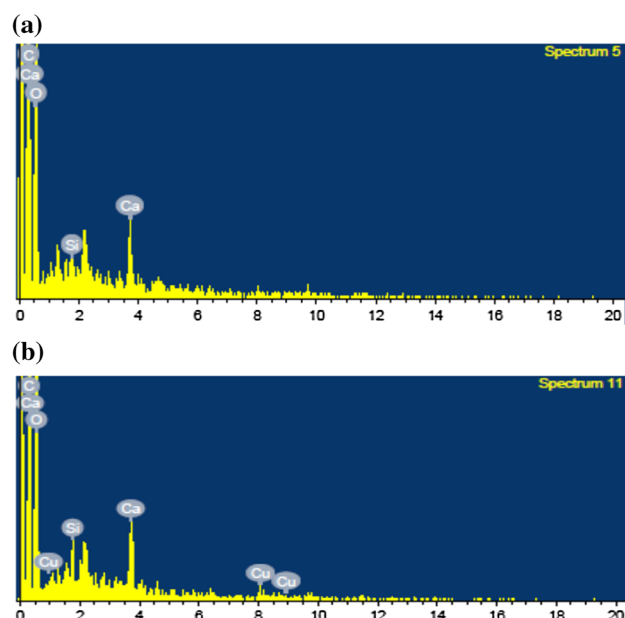


Fig. 3 EDS spectra of BF **a** before and **b** after adsorption of Cu(II)

concentration provides the driving force. The removal of Cu(II) as a function of contact time was studied at different concentrations (10, 30, 50, 70 and 100 mg L^{-1}). The contact time required for Cu(II) solutions with initial concentrations of 10, 30 and 50 mg L^{-1} to reach equilibrium was 10 min (Fig. 5). When initial Cu(II) concentration was increased to 70 and 100 mg L^{-1} , the equilibrium time increased to 30 min. Various adsorbents follow the basic principle of adsorption that the transfer of metal ions to the surface of the adsorbent increases with increase in concentration of metal ions and as the contact time increases it gradually decreases until it attains equilibrium as the adsorption sites of the adsorbent earlier free are now occupied. The adsorption capacity of Cu(II) at equilibrium was found to be 0.96, 2.98, 4.9, 6.83 and 9.84 mg g^{-1} , respectively at 10, 30, 50, 70 and 100 mg L^{-1} initial Cu(II) concentration. The equilibrium time of 30 min is reasonable being an economically favorable condition for the adsorbent used in this study. Based on these results, a contact time of 30 min was maintained for all subsequent batch experiments.

Table 1 EDS analysis of BF before and after adsorption of Cu(II)

Elements	Before Cu(II) adsorption		After Cu(II) adsorption	
	Weight (%)	Atomic (%)	Weight (%)	Atomic (%)
C	55.80	63.05	51.68	59.71
O	43.10	36.56	45.26	39.26
Si	0.11	0.05	0.62	0.31
Ca	0.99	0.34	1.47	0.51
Cu	–	–	0.96	0.21

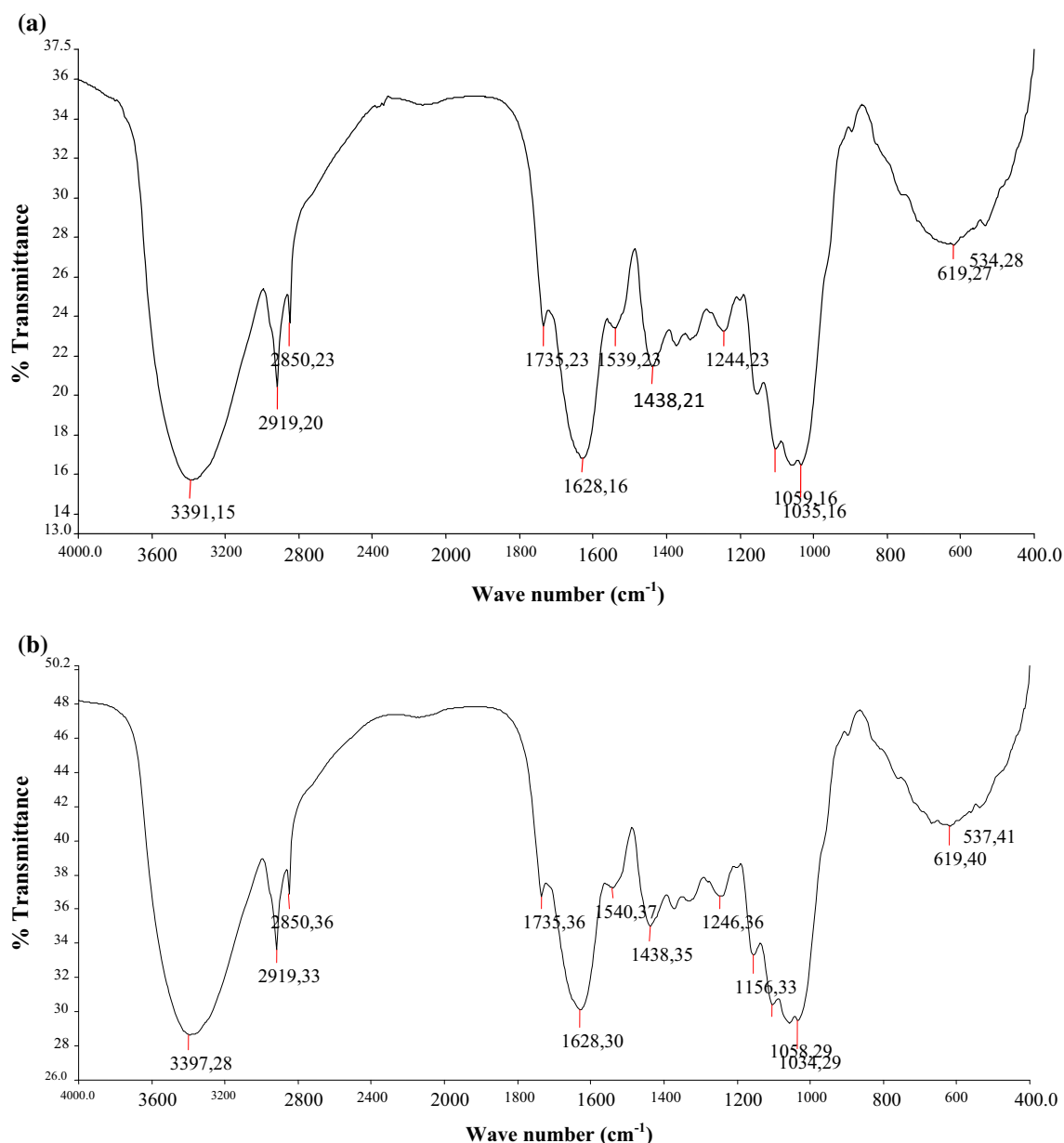


Fig. 4 **a** FTIR spectra of BF before Cu(II) adsorption, **b** FTIR spectrum of BF after Cu(II) adsorption

Effect of pH on adsorption

The effect of pH on the adsorption of Cu(II) is shown in Fig. 6. The % adsorption was minimum (54 %) at pH 2. The % adsorption reached maximum (96 %) when initial pH was increased to 4 and then remained almost constant up to pH 10. The surface charge of the adsorbent and speciation of Cu(II) is responsible for variation in the percent adsorption with respect to pH. At low pH values (1–2) the excess of H⁺ ions competes with Cu²⁺

ions resulting in least adsorption of Cu(II) and so the final pH of the solution remained unaffected. However, when initial pH of the solution was increased to 4, the % adsorption increased and reached to a maximum value (96 %) because of less competition between H⁺ and Cu²⁺ ions and final pH 4 remained almost constant. However, when pH of the solution was increased to 6, the % adsorption remained constant but final pH of the solution was decreased to 5. This is because at this pH, Cu(II) existed in the form of Cu²⁺ and Cu(OH)⁺ species

Fig. 5 Effect of contact time on adsorption of Cu(II) on BF at different concentrations (conditions; adsorbent = 0.2 g, pH 4, temperature = 30 °C)

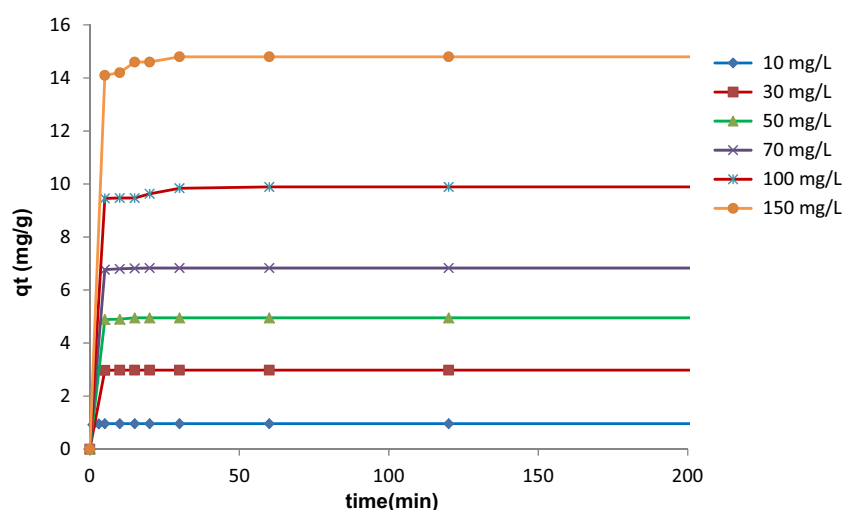
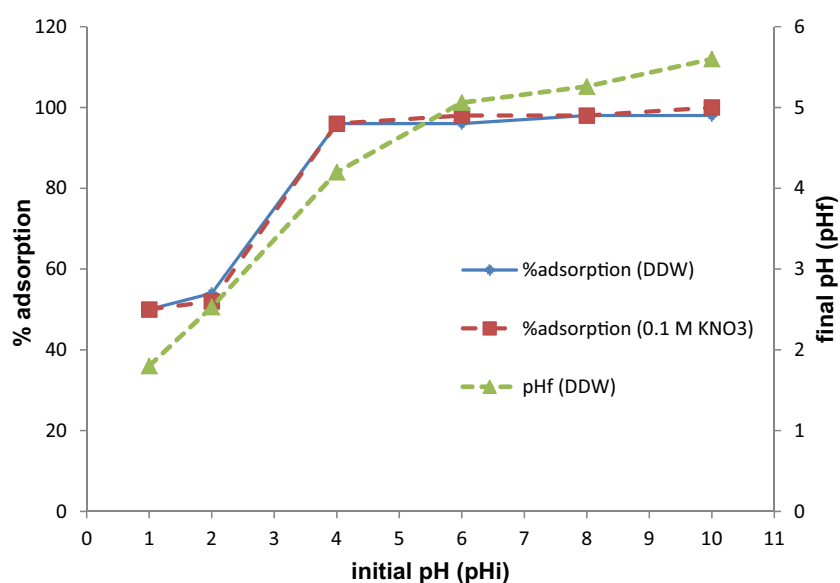


Fig. 6 Effect of pH and electrolyte on the adsorption of Cu(II) on BF (conditions; adsorbent = 0.2 g, Cu(II) = 50 mg L⁻¹, temperature = 30 °C)



(Zhong et al. 2014). Thus it was observed that adsorption of Cu(II) occurred in the form of Cu^{2+} and $\text{Cu}(\text{OH})^+$ at pH 6 and hence final pH of the solution was decreased. When pH of the solution was further increased to 10 the % adsorption of Cu(II) remained maximum. This might be due to the formation of $\text{Cu}(\text{OH})_2$ which is the dominant species above pH 6.3 and Cu(II) was adsorbed in the form of micro precipitation $[\text{Cu}(\text{OH})_2]$ on the surface and hence final pH of the solution further decreased to 5.5. However, the effect of electrolyte (0.1 M KNO_3) was negligible on the adsorption of Cu(II). The point of zero charge of the adsorbent was found to be 4 indicating that the surface of the adsorbent was positive at $\text{pH} < 4$, neutral at $\text{pH} 4$ and negative at $\text{pH} > 4$ (Fig. 7).

Adsorption isotherm models

The characteristics of the adsorbate and the adsorbent interactions are essentially understood through adsorption isotherms. Adsorption isotherms are of utmost importance so as to determine the design of adsorption systems as they give the surface characteristics of the adsorbent at micro level as well as the adsorption characteristics such as adsorption capacity, adsorption strength and adsorption state.

Langmuir adsorption isotherm

The equilibrium adsorption isotherms of homogeneous surfaces are determined by the theoretical Langmuir

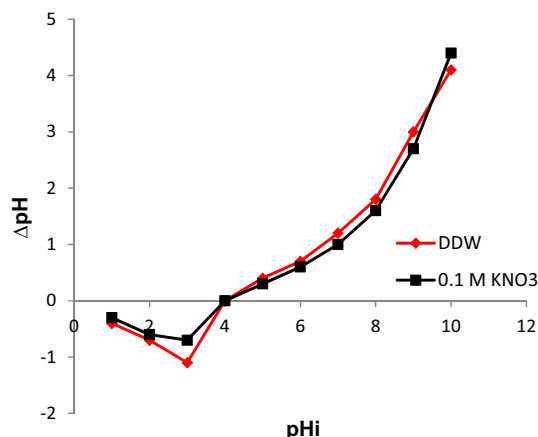


Fig. 7 Point of zero charge

isotherm model. This isotherm model is based on the assumption that all sites possess equal affinity for the adsorbate. The adsorption reaches to its maximum after a complete monolayer formation of adsorbate molecules onto the adsorbent surface according to this theory (Muresan et al. 2011). Mathematically the linear equation can be written as follows:

$$\frac{1}{q_e} = \frac{1}{q_m} \times \frac{1}{b} \times \frac{1}{C_e} + \frac{1}{q_m} \quad (2)$$

Where C_e is the equilibrium concentration of adsorbent (mg L^{-1}), q_e is the adsorption capacity (mg L^{-1}), b (L mg^{-1}) and q_m (mg g^{-1}) are Langmuir constants. The constant b is related to binding energy with a pH dependent equilibrium constant and q_m is maximum adsorption capacity in an ideal monolayer system. The plots between $1/q_e$ and $1/C_e$ gave straight lines, at 30, 40 and 50 °C (Figure not shown). The values of b and q_m were calculated from the slope and intercept (Table 2). The Langmuir model for this study was concluded to be best at 30 °C with r^2 value of 0.97.

Freundlich adsorption isotherm

The Freundlich equation is the empirical aspect for adsorbent with heterogeneous adsorbing surface and fits well for the adsorption of single solute within a fixed range of concentration (Hasan et al. 2008). The mathematical expression of the model is given as follows:

$$\log q_e = \log K_F + \frac{1}{n} \log C_e \quad (3)$$

where $1/n$ is a numerical value related to the adsorption intensity which varies with the heterogeneity, and K_F indicates the adsorption capacity. The plot of $\log q_e$ versus $\log C_e$ (Figure not shown) generated straight lines at different temperatures. As observed in Table 2, the value of

n was more than unity which indicated favorable adsorption of Cu(II), on the surface of the adsorbent. The value of n for Cu(II) was 1.53 and the r^2 value was 0.93 at 30 °C.

Tempkin isotherm model

Tempkin equation explains the factors which are explicitly responsible for adsorbate-adsorbent interactions. The Tempkin isotherm model is based on two assumptions, viz., heat of adsorption would decrease linearly rather than logarithmic with the coverage, and its derivation is characterized by a uniform distribution of binding energies up to some maximum binding energy (Dada et al. 2012). The Tempkin isotherm equation is given as:

$$q_e = B \ln A + B \ln C_e \quad (4)$$

where $B = RT/b$ and A (L mg^{-1}) are Tempkin constants for the equilibrium binding. The plot of q_e versus $\ln C_e$ at 30, 40 and 50 °C gave the straight lines (Figure not shown) and values of A and B were calculated from the intercept and slope, respectively (Table 2). The regression coefficient value (r^2) for Tempkin isotherm model at 30 °C being 0.99 confirmed better applicability of the equilibrium data as compared with Freundlich isotherm model at the same temperature.

Thermodynamics studies

The Van't Hoff equation,

$$\log K_c = \frac{\Delta S^\circ}{2.303R} - \frac{\Delta H^\circ}{2.303RT} \quad (5)$$

was used to determine the thermodynamics parameters like standard enthalpy change (ΔH°) and standard entropy change (ΔS°) obtained from the slope and intercept of the linear plot of $\log K_c$ versus $1/T$ as shown in Fig. 8. 30, 40, and 50 °C temperature regimes were used for this study. Equilibrium constant (K_c) was calculated at different temperatures using following relations

$$K_c = \frac{C_{Ac}}{C_e} \quad (6)$$

where C_{Ac} and C_e are the equilibrium concentrations of Cu(II) (mg L^{-1}) on adsorbent and in solution, respectively.

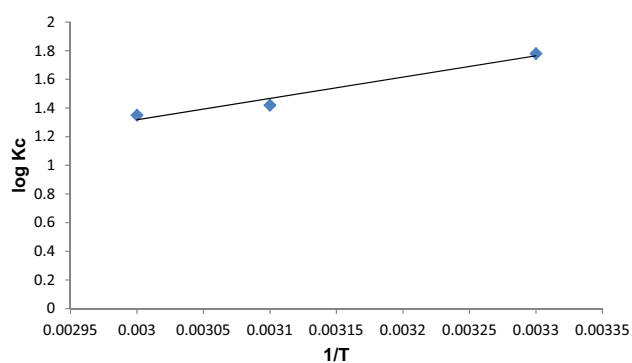
Standard free energy changes (ΔG°) at different temperatures were calculated from the relation:

$$\Delta G^\circ = -RT \ln K_c \quad (7)$$

Where R ($\text{JK}^{-1}\text{mol}^{-1}$) is the gas constant, T (K) is absolute temperature and ΔG° is the standard free energy change. The values of the parameters for thermodynamic studies are given in the Table 3. Exothermic nature of adsorption was shown by the negative value of ΔH° . The

Table 2 Adsorption isotherm parameters for adsorption of Cu(II) on BF at 30°, 40° and 50 °C

Isotherm models	Parameters	Temperature		
		30 °C	40 °C	50 °C
Langmuir	q_m (mg g ⁻¹)	27.03	27.02	37.04
	b (L mg ⁻¹)	0.26	0.31	0.09
	r^2	0.97	0.96	0.93
Freundlich	K_f (mg g ⁻¹)	5.16	6.53	2.96
	n	1.53	3.80	1.04
	r^2	0.93	0.42	0.88
Tempkin	A (L g ⁻¹)	4.58	4.86	1.79
	B (J mol ⁻¹)	3.79	4.21	4.99
	r^2	0.99	0.95	0.74

**Fig. 8** Van't Hoff plot

free energy change, ΔG° of the process increased with increase in temperature which concludes that the adsorption of Cu(II) was spontaneous and decrease in temperature favored the process. The negative value of ΔS° indicated decrease in entropy which might be due to decrease in randomness because of the fixation of Cu(II) ions onto adsorbent surface.

Adsorption kinetics

To carry out the kinetic studies of adsorption of Cu(II) the initial Cu(II) concentration was varied at constant temperature (30 °C). The data obtained were fitted in pseudo-first-order, pseudo-second-order and Weber–Morris intra-particle kinetics models. To confirm the applicability of the models with the experimental data, the parameters of kinetic models and regression coefficient values (r^2) were calculated. The results are presented in Table 4. The linear plots of the kinetic models for the adsorption of Cu(II) ions are shown in Fig. 9a–b.

Table 3 Thermodynamic parameters for the adsorption of Cu(II) on BF at different temperatures

Temperature (°C)	K_c	ΔH° (KJ mol ⁻¹)	ΔG° (KJ mol ⁻¹)	ΔS° (KJ mol ⁻¹ K ⁻¹)
30	61.5	-28.43	-10.35	-0.06
40	26.7		-8.53	
50	22.8		-8.37	

Lagargren pseudo-first-order kinetic model

A kinetic model for the adsorption analysis that is preceded by diffusion through a boundary will most likely follow the pseudo-first-order equation of Lagargren (Ofomaja et al. 2010);

$$\log (q_e - q_t) = \log q_e - \left(\frac{K_1}{2.303} \right) \times t \quad (8)$$

Where q_e is the amount of Cu(II) adsorbed per unit weight of the adsorbent at equilibrium (mg g⁻¹), q_t is the amount of Cu(II) adsorbed per unit weight of the adsorbent at any time t . K_1 is the pseudo-first-order rate constant. Linear plots between $\log (q_e - q_t)$ versus t gave the values of K_1 at different Cu(II) concentrations (Fig. 9a).

Pseudo-second-order kinetic model

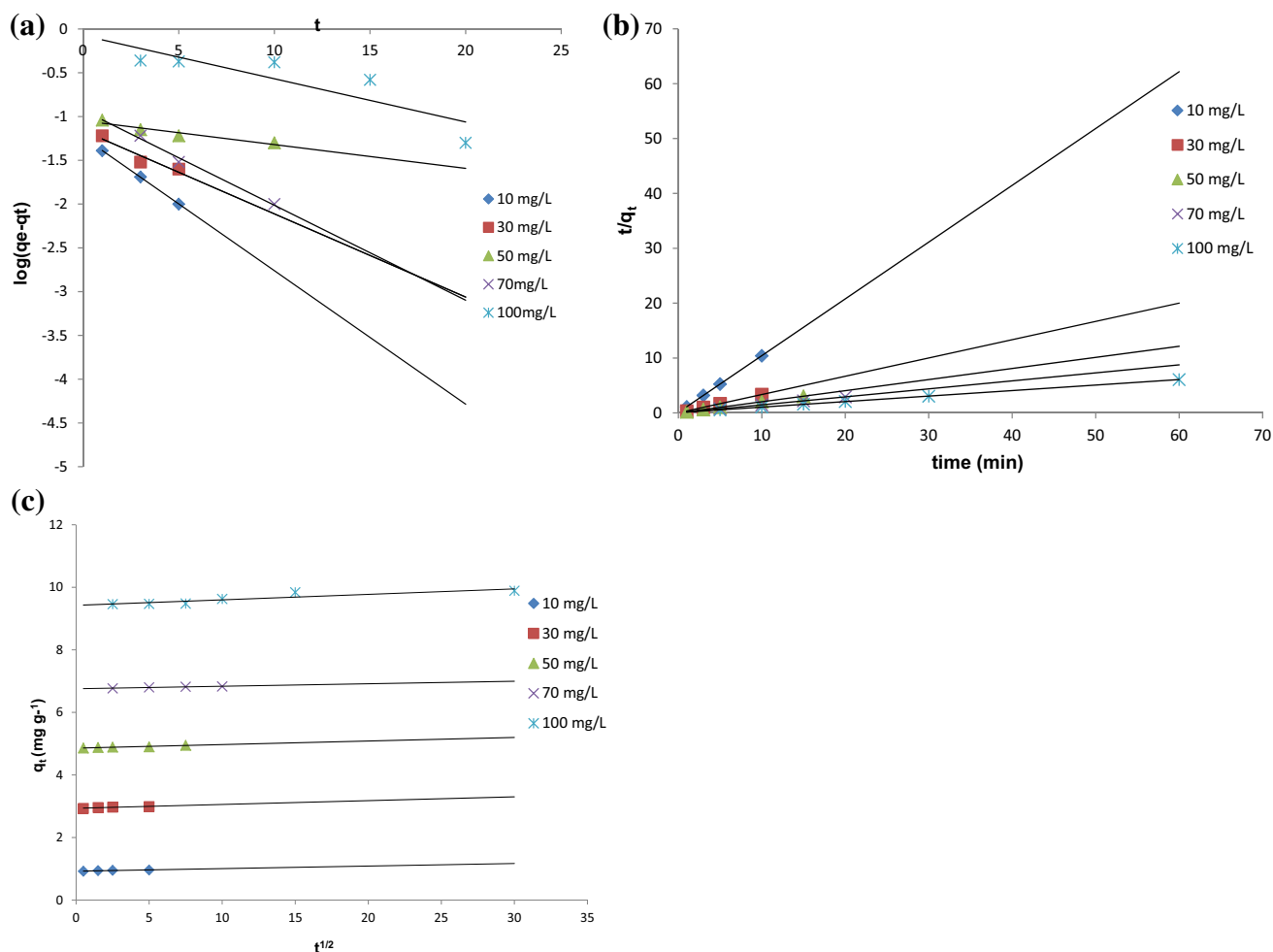
The adsorption is related to the squared product of the difference between the number of the equilibrium absorptive sites available on adsorbent and that of the occupied sites in the pseudo-second-order kinetic model. This model is expressed as follows (Monier et al. 2010);

$$\frac{t}{q_t} = \frac{1}{k_2 q_e^2} + \left(\frac{1}{q_e} \right) \times t \quad (9)$$

Where q_t (mg g⁻¹) amount of metal ions adsorbed onto the surface of the adsorbent at time t , K_2 is the pseudo-second-order rate constant (g mg⁻¹ min⁻¹) and q_e (mg g⁻¹) is the amount of Cu(II) adsorbed at equilibrium. The linear plots of t/q_t versus t which is given in (Fig. 9b) were used to calculate the pseudo-second-order constants. Table 4 showed that, the values of theoretical adsorption capacity q_e (cal) and experimental values q_e (exp) were very near for pseudo-second-order kinetics while these values were different for pseudo-first-order kinetics model. Thus the similar values for q_e (cal) and q_e (exp) and higher value of regression coefficient ($r^2 = 1$) than the pseudo-first-order model ($r^2 = 0.89$) indicated better applicability of pseudo-second-order kinetics model.

Table 4 Kinetics parameters for the adsorption of Cu(II) on BF

Kinetic models	Parameters	Concentration (mg L ⁻¹)				
		10	30	50	70	100
Pseudo-first-order	q_e (mg g ⁻¹) (exp)	0.96	2.99	4.95	6.83	9.89
	q_e (mg g ⁻¹) (cal)	0.06	0.07	0.09	0.12	0.84
	K_1 (min ⁻¹)	0.35	0.22	0.06	0.25	0.11
	r^2	0.99	0.89	0.91	0.97	0.74
Pseudo-second-order	q_e (mg g ⁻¹) (exp)	0.96	2.99	4.95	6.83	9.89
	q_e (mg g ⁻¹) (cal)	0.97	3.00	4.95	6.89	10
	K_2 (g mg ⁻¹ min ⁻¹)	16.39	12.34	10.20	4.22	0.21
	r^2	1	1	0.99	1	0.99
Intra-particle diffusion	K_{id} (mg g ⁻¹ min ^{-1/2})	0.01	0.01	0.001	0.008	0.017
	I	0.92	2.93	4.86	6.75	9.42
	r^2	0.85	0.88	0.93	0.95	0.81

**Fig. 9** **a** Pseudo-first-order kinetics model for the adsorption of Cu(II) on BF (conditions; adsorbent = 0.2, pH 4, temperature = 30 °C), **b** pseudo-second-order kinetics model for theadsorption of Cu(II) on BF (conditions; adsorbent = 0.2, pH 4, temperature = 30 °C), **c** intra-particle diffusion model (conditions; adsorbent = 0.2, pH 4, temperature = 30 °C)

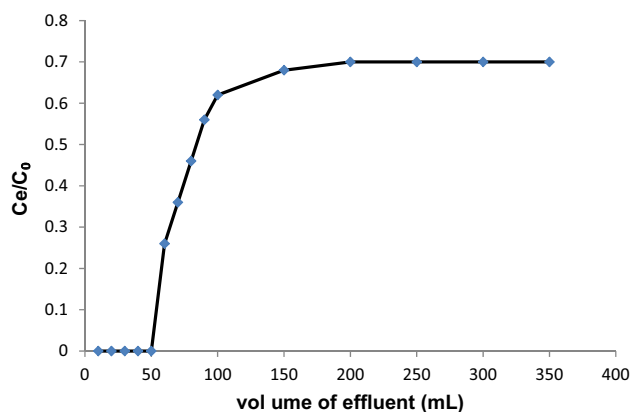


Fig. 10 Breakthrough capacity curve for adsorption of Cu(II) on BF (conditions; adsorbent = 0.2 g, Cu(II) = 50 mg L⁻¹, flow rate = 1 mL min⁻¹, temperature = 30 °C)

Weber–Morris intra-particle diffusion model

This model can be expressed as;

$$q_e = k_{id} \times t^{1/2} + I \quad (10)$$

Where K_{id} is the intra-particle diffusion rate constant (mg g⁻¹ min^{-1/2}) and I (mg g⁻¹) is the constant of intra-particle diffusion model. The plot of q_t versus $t^{1/2}$ at different initial Cu(II) concentrations gave the value of K_{id} (Fig. 9c). The r^2 values obtained for the adsorption of Cu(II) were not sufficiently high, indicating the intra-particle diffusion model was not better fitted. The constant I could be attributed to boundary layer thickness. By increasing initial Cu(II) concentration, I value was increased which indicated the enhancement of mass transfer resistance through the boundary layer (Raji and Pakizeh 2014). The parameters calculated are given in Table 4.

Breakthrough studies

The Breakthrough capacity determination is important as it directly affects the feasibility and economics of the process (Volesky 2003). It was observed that 50 mL of Cu(II) solution containing 50 mg L⁻¹ Cu(II) could be passed through the column without detecting Cu(II) in the effluent. The breakthrough curve for 50 mg L⁻¹ initial Cu(II) concentration and flow rate of 1 mL min⁻¹ with 0.2 g adsorbent is shown in Fig. (10). The breakthrough capacity and exhaustive capacities were found to be 12.5 and 37.5 mg g⁻¹, respectively.

Desorption studies

From the solid waste management point of view, the desorption of adsorbed metal and concentrating the metal in

minimum volume is necessary. Thus, to make the process more economical and feasible desorption studies were carried out. Desorption studies were done for single metal system in a continuous flow column (0.6 cm internal diameter) by using 0.1 M HCl as a desorbing solution. The adsorption of Cu(II) with 50 mg L⁻¹ initial concentration in single metal system was 96.2 and 93.33 % of Cu(II) was desorbed within 40 mL effluent.

Conclusion

Boston fern also called as sword fern is a perennial ornamental plant abundantly available in India. It has better capability and efficacy for the removal of copper from aqueous medium. The order of adsorption of various heavy metals on Boston fern was Cu(II) > Pb(II) > Ni(II) > Cd(II) > Cr(VI). The maximum adsorption occurred at pH 4. The regression coefficient values (r^2) suggest that the equilibrium data fitted well to Langmuir, Freundlich and Tempkin adsorption isotherms at 30 °C. The adsorption process was found to be exothermic and spontaneous in nature. Better applicability of pseudo-second-order rate equation was confirmed by kinetics model. Breakthrough capacity showed that 50 mL of Cu(II) solution containing 50 mg L⁻¹ Cu(II) could be passed through the column without detecting Cu(II) in the effluent. Desorption studies showed that 93.33 % of Cu(II) could be recovered within 40 mL of the effluent by using 0.1 M HCl solution by column operation.

Acknowledgments The authors gratefully acknowledge the Chairman, Department of Applied Chemistry for providing facilities to conduct the present study, University sophisticated instrumentation facility (USIF), Aligarh Muslim University, Aligarh and Sophisticated analytical instrumentation facility (SAIF) Punjab University, Chandigarh for the analysis of data and University Grants Commission for providing financial assistance in the form of Non-Net UGC Fellowship.

Open Access This article is distributed under the terms of the Creative Commons Attribution 4.0 International License (<http://creativecommons.org/licenses/by/4.0/>), which permits unrestricted use, distribution, and reproduction in any medium, provided you give appropriate credit to the original author(s) and the source, provide a link to the Creative Commons license, and indicate if changes were made.

References

- Ahalya N, Ramachandra TV, Kanamadi RD (2003) Biosorption of Heavy Metals. Res. J. Chemistry and Environ 7(4)
- Al-Asheh S, Banat F, Abu-Aitah L (2003) Adsorption of phenol using different types of activated bentonites. Sep Purif Technol 33(1):1–10

- Antunes PM, Watkins GM, Duncan JR (2001) Batch studies on the removal of gold (III) from aqueous solution by *Azolla filiculoides*. Biotechnol Lett 23:249–251
- Bulut Y, Tez Z (2007) Adsorption studies on ground shells of hazel nut and almond. J Hazard Mater 149:35–41
- Corapcioglu MO, Huang CP (1987) The adsorption of heavy metals onto hydrous activated carbon. Water Res 21:1031–1044
- Dada AO, Olalekan AP, Olatunya AM, Dada O (2012) Langmuir, Freundlich, Tempkin and Dubinin-Radushkevich isotherms studies of equilibrium sorption of Zn^{2+} unto phosphoric acid modified rice husk. J App Chem 3:38–45
- Donmez G, Aksu Z, Ozturk A (1999) A comparative study on heavy metal adsorption characteristics of some algae. Process Biochem 34:885–892
- Elangovan R, Philip L, Chandraraj K (2008) Adsorption of chromium species by aquatic weeds: kinetics and mechanism studies. J Hazard Mater 152:100–112
- Eligwe CA, Okaolue NB, Nwambu CO, Nwoko CIA (1999) Adsorption thermodynamics and kinetics of mercury (II), cadmium (II) and lead (II) on lignite. Chem Eng Technol 22:45–49
- Gupta VK, Ali I (2000) Utilisation of bagasse fly ash (a sugar industry waste) for the removal of copper and zinc from wastewater. Sep Purif Technol 18:131–140
- Hasan M, Ahmad AL, Hameed BH (2008) Adsorption of reactive dye onto cross linked chitosan oil palm ash composite beads. Chem Eng J 136:164–172
- Hasany SM, Ahmad R, Chaudhary MH (2003) Investigation of sorption of Hg(II) ions onto coconut husk from aqueous solution using radiotracer technique. Radiochim Acta 91:533–538
- Ho YS, Huang CT, Huang HW (2002) Equilibrium sorption isotherm for metal ions on tree fern. Process Biochem 37:1421–1430
- Igbinsola EO, Okah AI (2009) Impact of discharge waste water effluents on the pH physico-chemical qualities of a receiving water shed in a typical rural community. Int J Environ Sci Tech 6:175–182
- Issabeayev G, Aroua MK, Sulaiman NMN (2006) Removal of lead from aqueous solutions on palm shell activated carbon. Bioresour Technol 97:2350–2355
- Khalid N, Ahmad S, Kiani SN, Ahmad J (1999) Removal of mercury from aqueous solution by adsorption to rice husks. Sep Sci Technol 34:3139–3153
- Kiyohara T, Anazawa K, Sakamoto H, Tomiyasu T (2003) Adsorption of mercury on used tea leaves and coffee beans. Bunseki Kagaku 52:227–230
- Lodenius M, Seppanen A, Uusi Rauva A (1983) Adsorption and mobilization of mercury in peat soil. Chemosphere 12:1571–1581
- McKay G (2000) The kinetic of sorption of divalent metal ions onto sphagnummoss peat. Water Res 34:735–742
- Monier M, Ayad DM, Sarhan AA (2010) Adsorption of Cu(II) and Hg(II) and Ni(II) ions by modified natural wood chelating fibres. J Hazard Mater 176:348–355
- Murugesan A, Ravikumar L, Sathiyasalvabala V, Senthikumar P, Vidhyadevi T, Kirupha DS (2011) Removal of Pb(II), Cu(II) and Cd(II) ions from aqueous solution using polyazomethineamides: equilibrium and kinetic approach. Desalination 271:199–208
- Navarro RR, Sumi K, Fujii N, Matsumura M (1996) Mercury removal from waste water using porous cellulose carrier modified with polyethyleneimine. Water Res 30:2488–2494
- Ofomaja AE, Naidoo EB, Modise SJ (2010) Kinetic and pseudo-second-order modeling of lead adsorption onto pine cone powder. J Ind Eng Water Res 49:2562–2572
- Periasamy K, Namasivayam C (1996) Removal of copper (II) by adsorption onto peanut hull carbon from water and copper plating industry wastewater. Chemosphere 32:769–789
- Ponomarev AV, Bludenko AV, Makarov IE, Pikaev AK, Kim DK, Kim Y, Han B (1997) Combined electron beam and adsorption purification of water from mercury and chromium using materials of vegetable origin as sorbents radiant. Phys Chem 49:473–476
- Raji F, Pakizeh M (2014) Kinetic and thermodynamic studies of Hg(II) adsorption onto MCM-41 modified by $ZnCl_2$. Appl Surf Sci 301:568–575
- Sheng PX, Tan LH, Chen JP, Ting YP (2004) Biosorption performance of two brown marine algae for removal of chromium and cadmium. J Dispers Sci Technol 25:679–686
- Taghi Ganji M, Khosravi M, Rakhshae R (2005) Adsorption of Pb, Cd, Cu and Zn from the wastewater by treated *Azolla filiculoides* with $H_2O_2/MgCl_2$. Int J Environ Sci Technol 1:265–271
- Tripathy SS, Kanungo SB (2005) Adsorption of Co^{2+} , Ni^{2+} , Cu^{2+} and Zn^{2+} from 0.5 M NaCl and major ion sea water on a mixture of δ - MnO_2 and amorphous FeOOH. J Colloid Interface Sci 284:30–38
- Vanquez G, Gonzalez-Alvarez J, Freire S, Lopez-Lorenzo L, Antorrena G (2002) Removal of cadmium and mercury ions from aqueous solution by sorption on treated *Pinus pinaster* bark: Kinetics and isotherms Bioresour Technol 82:247–251
- Volesky B (2003) Sorption and Biosorption. BV Sorbex Inc, Montreal
- Yuh-shan HO (2002) Removal of copper ions from aqueous solution by tree fern. Water Res 37:2323–2330
- Zhong Q, Yue Q, Li Q, Gao B, Xu X (2014) Removal of Cu(II) and Cr(VI) from waste water by an amphoteric sorbent based on cellulose- rich biomass. Carbohydr Polym 111:788–796